



All-Inkjet-Printed Humidity Sensors for the Detection of Relative Humidity in Air and Soil—Towards the Direct Fabrication on Plant Leaves

Walid Ait-Mammar¹, Samia Zrig¹, Nathalie Bridonneau¹, Vincent Noël¹, Eleni Stavrinidou², Benoît Piro¹, Giorgio Mattana^{1,*}

¹ Sorbonne Paris Cité, ITODYS, UMR 7086 CNRS, Univ. Paris Diderot, 15 rue J-A de Baïf, Cedex 13 75205 Paris, France

²Laboratory of Organic Electronics, Department of Science and Technology, Linköping University, SE-601 74, Norrköping, Sweden

*corresponding author: giorgio.mattana@univ-paris-diderot.fr

ABSTRACT

We demonstrate the fabrication, by exclusive means of inkjet-printing, of capacitive relative humidity sensors on flexible, plastic substrate. These sensors can be successfully used for the measurement of relative-humidity in both air and common soil. We also show that the same technique may be used for the fabrication of the same type of sensors on the surface of the leaves of *Elægnus Ebbingei* (silverberry). Our results demonstrate the suitability of leaves as substrate for printed electronics and pave the way to the next generation of sensors to be used in fields such as agriculture and flower farming.

INTRODUCTION

Global warming may be defined as the anthropogenic, anomalous increase of average global temperatures at the fastest recorded rate in human history¹. The causes of this phenomenon are various and quite complex but two major contributions have been identified so far, namely deforestation and the release in the atmosphere of greenhouse gases mostly related to industrialization². Global warming typically manifests itself as a series of heat and cold waves³ with disastrous consequences for both agriculture and flower farming. Assuming 2°C of warming within 2060, it has been recently estimated that the developed countries may experience an average decrease of their Gross Domestic product (GDP) of 0.3 % per annum but this loss could be ten times higher if, as less conservative forecasts predict, temperature increase reaches 5°C⁴.

Relative humidity (RH) is one of the most important parameters regulating plants growth⁵. It has been shown that when soil RH goes below a critical threshold value (depending mostly on the plant species and stage of development) plants experience a series of negative effects collectively known as “drought stress”⁶. Drought stress reduces leaf size, stem extension and root proliferation and, as such, requires prompt and careful management as it can seriously compromise plants blooming as well as seeds and fruits production⁷. This issue becomes particularly critical if one considers the fact that nowadays plantations are more and more often exposed to dangerous fluctuations of RH caused by the aforementioned climatic instability⁸. RH sensing systems capable of allowing real-time monitoring of humidity at different levels (atmosphere and soil) are therefore strongly needed if, within the context of global warming, one aims at reducing the damage caused by plants exposure to dehydration.

Ideally, these sensors should be precise, cheap and exhibit low power consumption⁹. Light weight and flexibility are other desirable characteristics¹⁰. Most of these requirements may be met by fabricating RH sensors on thin plastic films by using printing techniques. The inkjet-printing technique, in particular, has attracted considerable attention for the manufacture of this type of sensors because it is an additive, contactless and digital technique allowing devices fabrication at ambient conditions and the rapid prototyping of different structures and designs¹¹. Several examples of inkjet-printed RH sensors fabricated on flexible, plastic substrates have been reported so far in the literature^{11–13}. All these examples describe devices intended for ambient RH monitoring. Surprisingly, very few papers report on the utilization of such sensors for RH measurements in soil. To the best of our knowledge, the only example published so far concerns a sensing platform called SenSprout and consisting of inkjet-printed sensors for humidity detection in air and in soil, fabricated on a paper substrate^{14,15}. Unfortunately, these papers report very little on the sensors characterization so that their performances remain mostly unknown.

In the present work, we report on the fabrication of all-inkjet-printed RH sensors fabricated on flexible, plastic foils. Sensors calibration and dynamic characterization are fully described as well as their utilization for soil moisture measurements. Finally, we present preliminary results demonstrating the possibility of using the same fabrication technique to manufacture the sensors directly on the surface of leaves. This is presumably the first example ever reported on the employment of plant leaves as a substrate for inkjet-printing.

MATERIALS AND METHODS

Substrates

Kapton® Type HN (purchased from Dupont, 125 µm) was used as a substrate for the fabrication of the RH sensors thanks to its excellent thermal stability and chemical resistance to solvents¹⁶.

The leaves used as substrates were taken from *Elægnus Ebbingei* plants (silverberry) and used immediately after cutting with no further treatments.

Inks for inkjet-printing

The sensors electrodes were fabricated using a commercially available inkjet-printable Ag nanoparticles-based ink (Sicrys™ I40TM-106, by Pv NanoCell, metal loading: 40 % wt).

Cellulose acetate butyrate (CAB, average $M_n \sim 12,000 \text{ g}\cdot\text{mol}^{-1}$, purchased from Sigma-Aldrich) was used as RH sensing layer because of its good solubility in a large variety of organic solvents compatible with the printer cartridges^{17,18} and its good performances resulting in a low hysteresis in the sensors calibration curve¹⁹. The CAB ink was prepared according to an already published procedure¹²: 65 mg of CAB powder were dissolved overnight in 4 mL of hexyl acetate (purchased from Sigma Aldrich) and the solution (dynamic viscosity of around 10 cP) was used without filtration.

For the inkjet-printing on leaves, an inkjet-printable aqueous suspension of poly(3,4-ethylenedioxythiophene)-poly(styrenesulfonate) (PEDOT:PSS) (Orgacon™ IJ-1005, from Sigma Aldrich) was also used for the fabrication of the sensors electrodes.

Sensors fabrication

General considerations

For RH measurements, a capacitive structure was chosen as, compared to other possible types of sensors (for instance resistive RH sensors) it presents a few advantages such as higher robustness to ambient temperature variations²⁰ and smaller power consumption²¹.

The capacitive RH sensors were fabricated using an interdigitated electrodes configuration (IDE) where the two electrodes are shaped as a comb and lie on the same substrate and are covered by a thin layer of a RH sensing material; the main advantage of this configuration is that it allows direct exposure of the sensing layer to the analyte to be detected, which typically speeds up the sensors response²².

Sensors inkjet-printing on Kapton®

Kapton® foils were preliminarily cleaned with subsequent baths in acetone, isopropanol and deionized water then they were dried under argon flow. Prior to printing, substrates were heated at 180°C for 60 minutes to promote surface dehydration.

Inkjet-printing of the interdigitated electrodes was performed using a Dimatix DMP-2800 printer. Platen temperature was fixed at 40°C and cartridge temperature at 30°C; 10 pL cartridges were used and printing was carried out using a drop-spacing of 25 μm and a drop velocity of 7 $\text{m}\cdot\text{s}^{-1}$. The IDE comb was composed of 52 pairs of electrodes, each electrode had a nominal width of 50 μm and the nominal gap between two adjacent electrodes was set at 100 μm . Each comb was connected to a connection pad (2.5 mm \times 2.5 mm) and the sensor total active area was 15 mm \times 10 mm. Electrodes were fabricated by printing a single layer of silver ink and had a thickness of about 300 nm. After printing, sensors were annealed in a conduction oven at 180 °C for an hour, to allow solvent evaporation and Ag nanoparticles sintering.

Subsequently, the CAB solution was inkjet-printed on the top of the IDE comb. For CAB printing, the same temperatures as above were used; in this case, the drop-spacing was set at 30 μm and the drop velocity at 8 $\text{m}\cdot\text{s}^{-1}$. To ensure good electrodes covering and improve homogeneity, 24 layers of CAB were printed one on the top of the other, resulting in a final layer with an approximate thickness of 8 μm . After printing, sensors were annealed on a hot plate at 60 °C for 60 minutes to promote solvent evaporation. Figure 1A depicts a scheme describing the device geometry while Figure 1B presents two optical pictures of the IDE before and after CAB deposition.

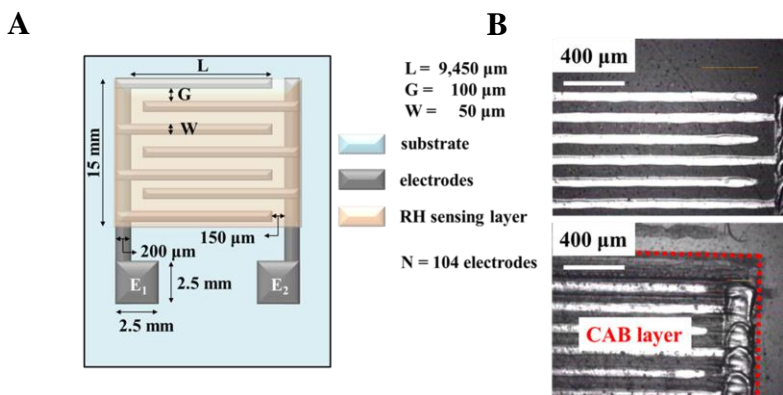


Figure 1. A) Scheme describing the capacitive RH sensor geometry. B) Top picture: silver IDE before CAB deposition. Bottom picture: IDE after CAB deposition.

Sensors inkjet-printing on leaves

Silverberry leaves were flattened and fixed on a rigid, flat substrate with the help of scotch tape. The smoother bottom face of the leaves was used for inkjet-printing. PEDOT:PSS was used in this case for the fabrication of the IDE. The platen was kept at 28 °C and the cartridge at 30 °C; drop-spacing was set at 15 μm and the drop velocity at 7 m.s⁻¹. Sensors fabricated directly on leaves were composed of 3 pairs of electrodes, each electrode had a nominal width of 100 μm and the nominal gap between two adjacent electrodes was set at 200 μm. The sensors total active area was 2 mm × 10 mm. Electrodes were fabricated by printing 6 layers of PEDOT:PSS (instead of 1 Ag layer on Kapton®) to obtain a conductive, homogeneous and visible layout, and had a thickness of about 1 μm. After printing, no thermal treatment was performed and the CAB sensing layer was deposited by following the same procedure as above. Sensors were then left at ambient conditions to dry for 24 hours before being tested (leaving the leaf bud in water to avoid dehydration). An optical image of the inkjet-printed humidity sensor fabricated on a leaf is shown in Figure 2.

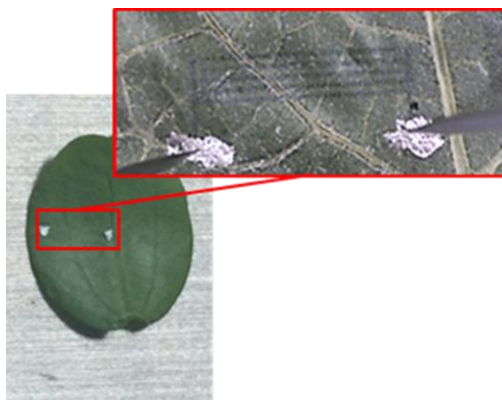


Figure 2. Figure 2. Optical image of an inkjet-printed RH sensor on a leaf (left). Inset: zoom on the sensor, the IDE is visible as well as two small drops of conductive silver paste and the probes used for measurements.

Sensors characterization

Electrical Impedance Spectroscopy (EIS)

Sensors were characterized at room temperature ($T = 25\text{ }^{\circ}\text{C}$) using an Agilent E4980A Precision LCR Meter. Frequency was swept between 10 kHz and 2 MHz, while applying a constant voltage of 1 V and a sinusoidal amplitude of 0.1 V. Prior to each measurement, open and short-circuit calibrations were performed.

Static characterization inside a climatic chamber

The devices static response was acquired inside a climatic chamber (Climacell, Fischer Bioblock Scientific). RH was swept between 20 and 90% with steps of 10 % (upsweep curve) and then brought back to 20 % (downsweep curve); temperature was kept constant at 25 °C and capacitance was measured using the same LCR meter described in the previous paragraph.

Dynamic characterization inside a gas mixing system

Dynamic measurements were performed inside a homemade gas mixing system. Devices were placed inside an electrochemical cell (volume: 15 cm³) having two inlets (one for dry argon, the other for saturated water in argon) and one outlet. Humidity was varied abruptly between 20 and 80% and the sensors' response over time was recorded using the Agilent E4980A Precision LCR Meter. RH inside the cell was monitored using a commercial humidity sensor (TRIXIE Thermo-hygrometer).

Dynamic characterization in soil

Common garden soil was used for such tests (silty soil, $5.0 \leq \text{pH} \leq 6.5$)²³; the soil was placed inside plastic pots and its humidity was varied by wetting with deionized water. RH values were checked using a commercial humidity sensor for soil (50PCS Egg Control Digital Plant Moisture Light Soil Humidity Meter).

For measurements in soil, the sensors were fixed on a plastic substrate and then inserted inside the earth at a depth of approximately 3 cm. The protocol used for dynamic measurements was the following:

- sensors were left in air for approximately 30 s;
- sensors were inserted inside the first soil pot and left there for approximately 150 s;
- sensors were then taken out from the pot immediately placed in the second soil pot.

The plateau values measured in soil were used to plot a capacitance vs RH curve (similar to the static curves obtained inside the climatic chamber).

RESULTS AND DISCUSSION

EIS results

The sensors presented in this paper may be, in a first approximation, described as a simple parallel RC circuit (see inset of Figure 3).²⁴ This model is used quite often in the literature as it allows a simple and rapid estimation of the sensors' capacitance; however, its validity is limited to the frequency range where the estimated capacitance remains constant. A typical example of capacitance vs frequency curve acquired on our inkjet-printed sensors is illustrated in Figure 3 with a capacitance plateau centered at

around 400 kHz; as a consequence, this frequency value was chosen to perform all the capacitance vs RH tests (moreover, this value is also compatible with read-out electronic circuits²⁵).

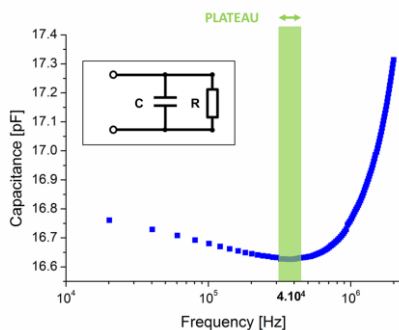


Figure 3. Example of capacitance vs frequency graph. Inset: equivalent circuit used to extract capacitance from impedance measurements

Static characterization

The sensors response was normalized with respect to the capacitance value at RH = 20 %. Figure 4 shows a statistic characterization on three different devices. The upsweep and downsweep curves do not overlap perfectly; such a phenomenon, called “hysteresis”, is typical of this type of devices and may be attributed to thermodynamic non-reversibility of the sensing layer swelling and de-swelling processes. Swelling of solid materials is a multi-step, out of equilibrium process. Local conformational reorganization of the polymeric matrix is often coupled to solvent molecule binding. It has been reported²⁶ that water absorption in cellulose and cellulose-based thin films causes a significant increase of the film surface area, as fibers swell and expose strongly hydrophilic sites (mostly – OH groups) to the aqueous vapor. The increase of cellulose surface area requires a preliminary step of intramolecular hydrogen bonds disruption: adsorption and desorption phenomena are therefore not energetically equivalent. The solid lines in Figure 4 represent a Boltzmann fit for both the upsweep and downsweep curves. The tested sensors show a typical sigmoidal response to relative humidity variations, widely documented for similar devices based on polymeric sensing films^{12,27}. Fitting is good for both curves ($R^2 > 0.99$) even if they clearly have different inflection points, thus further demonstrating that swelling and de-swelling are not energetically equivalent.

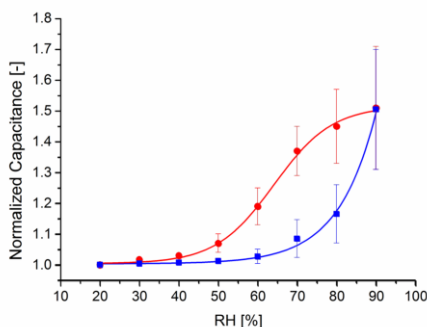


Figure 4. Static characterization (expressed in terms of normalized capacitance) on three different devices: ■ upsweep curve, ● downsweep curve. The solid lines represent Boltzmann fits (in both cases: $R^2 > 0.99$).

Dynamic characterization

An example of dynamic characterization on a single device is reported in Figure 5, where the relative variation of capacitance as a function of time was expressed as follows:

$$\Delta C_{\%}(t) = \frac{C(t) - C(0)}{C_{\max} - C(0)} \times 100$$

to obtain percentage values in the range from 0 to 100%. Dynamic measurements were used to estimate the sensors response (t_1) and relaxation times (t_2), here defined as the rising time from 10 to 90% of the final capacitance value and the falling time from 90 to 10 % of the final capacitance value, respectively. In all the tested samples ($N = 5$), response times were $t_1 < 100$ s while sensors relaxation was almost instantaneous, $t_2 < 5$ s. This data are in good agreement with results reported in the literature¹² on similar devices and are perfectly compatible with the final targeted application, as drought stress takes several tens of minutes to occur after RH has fallen below the critical threshold value. The difference between t_1 and t_2 may be explained in terms of the different kinetics of water adsorption and desorption²⁸: as cellulose interaction with water molecules is a multi-step process, the kinetically rate-limiting step can be different depending on the reaction direction.

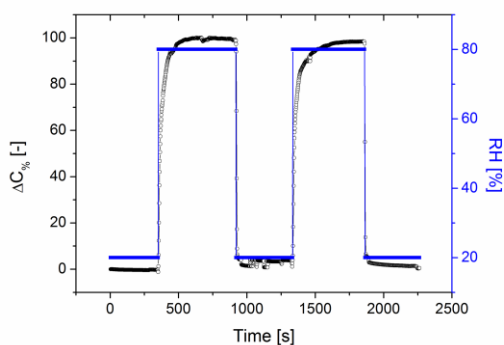


Figure 5. Example of a sensor dynamic response (○ capacitance percentage variation, ■ RH).

Characterization in soil

An example of dynamic characterization performed in soil is reported in Figure 6A. Figure 6B summarizes the normalized plateau values (with respect to RH = 37 %) in soil as a function of RH on a set of $N = 3$ sensors. Comparison with the values of RH provided by the commercial humidity sensor demonstrates that our inkjet-printed sensors exhibit excellent repeatability; reproducibility between different sensors is less good but becomes acceptable if one considers RH values lower than 50 %, which is the range targeted for the final application. As can be seen from Figure 6B, capacitance variations in soil are much stronger than those observed in air, and hysteresis is much smaller. These observations may be tentatively attributed to the fact that air and soil are two media characterized by a completely different dielectric behavior because of the soluble, electrolytic salt species normally present in soil^{30,31} (but absent in air) as well as because of the formation in soil of thin, liquid water films surrounding the mineral particles³² and coming in direct contact with the sensors cellulose layer.

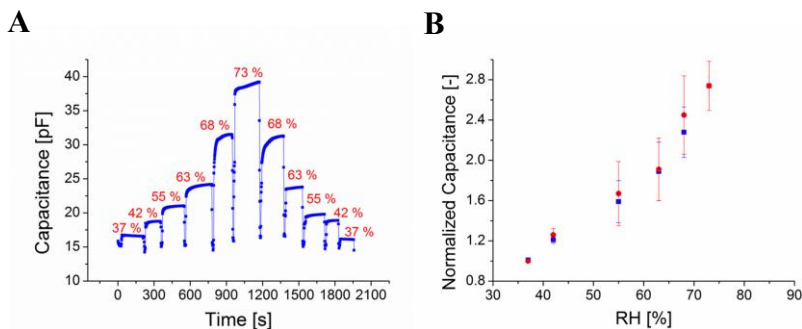


Figure 6. A) Example of a sensor dynamic characterization in soil; the red percentage values are the RH values displayed by the commercial sensor. B) Normalized static capacitance in soil (■ upsweep curve, ● downsweep curve).

Inkjet-printed sensors on leaves: proof of concept

Electrical connections on sensors printed on leaves were taken by putting two small drops of conductive silver paste on each IDE and by placing directly two probes on them (see Figure 2). Capacitance at 400 kHz and ambient conditions is around 0.01 pF, because of the low number of interdigitated fingers. Figure 7 shows an example of a sensor response to pulses (duration of 2 s) of saturated water vapor; between 300 and 400 s, the sensor was disconnected from the LCR meter to show the difference between its capacitive signal and electrical ground noise. While far from being optimized, these preliminary tests show that the inkjet-printed sensors fabricated on leaves are perfectly functional. The possibility of using these sensors to directly monitor plants transpiration is currently under investigation.

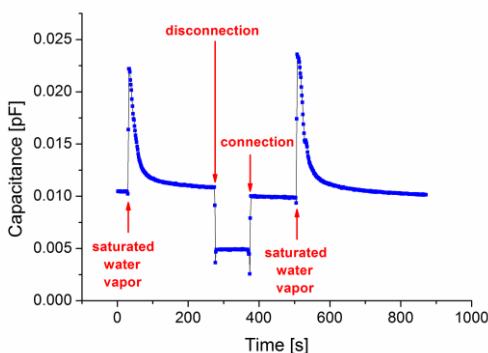


Figure 7. Dynamic response of a sensor inkjet-printed on a silverberry leaf.

CONCLUSION

In this paper, we presented a protocol for the fabrication of inkjet-printed, flexible capacitive RH sensors for measurements in air and in soil. These sensors show performances that are perfectly compatible with the final targeted application, i.e. the real

time monitoring of plants environmental conditions within a context of global warming and climate change that make plants often exposed to the risk of developing drought stress. By coupling the sensor with devices that deliver signaling molecules to the plants²⁹ one can envision enhancing the plant tolerance to drought.

Finally, we illustrated the first example of inkjet-printed RH sensor fabricated directly on the surface of a leaf thus demonstrating the compatibility between a living, vegetal substrate and the inkjet-printing deposition technique and materials. This last result could pave the way to a new generation of devices and sensing systems for agriculture and flower farming using plants directly as mechanical support.

ACKNOWLEDGMENTS

The authors gratefully acknowledge the financial support from the FET program within the Horizon 2020 Research and Innovation Program of the European Commission, under the HyPhOE FET-open project (grant agreement no. 800926).

References:

1. H. Uzawa, *Economic Theory and Global Warming*, (Cambridge University Press, New York, 2003), p. 21.
2. I. Dincer, C.O. Colpan and F. Kadioglu, *Causes, Impacts and Solutions to Global Warming*, (Springer Science & Business Media, New York, 2013) p. 17.
3. T. C. Peterson et al. B., *Am. Meteorol. Soc.* 12, 822 (2013).
4. K. Wade and M. Jennings, The impact of climate change on the global economy. Schroders Economics Team (2016).
5. L. M. Mortensen, *Sci. Hortic.* 29, 301-307 (1986).
6. L. E. Arve et al., in *Abiotic Stress in Plants - Mechanisms and Adaptations*, edited by A. Shanker and B. Venkateswarlu (IntechOpen, Rijeka, 2011) pp. 267-281.
7. M. Farooq et al., *Agron. Sustain. Dev.* 29, 185-212 (2009).
8. C. Aydinalp and M.S. Cresser, *American-Eurasian J. Agric. & Environ. Sci.* 3, 672-676 (2008).
9. Aqeel-ur-Rehman et al., *Comp. Stand. Inter.* 36, 263-270 (2014).
10. G. Mattana and D. Briand, *Mater. Today* 19, 88-99 (2016).
11. G. Mattana et al., *Adv. Mater. Technol.* 2, 1700063, (2017).
12. F. Molina-Lopez et al., *Sensor Actuat. B-Chem.* 166, 212-222 (2012).
13. G. Mattana et al., *IEEE Sens. J.* 13, 3901-3909 (2013).
14. Y. Kawahara et al., *Proc. UbiComp* 5-8 Sept. (2012).
15. S. Kim et al., Proceedings of the 43rd European Microwave Conference 7-10 Oct. (2013).
16. <https://www.dupont.com/content/dam/dupont/products-and-services/membranes-and-films/polyimide-films/documents/DEC-Kapton-summary-of-properties.pdf> (accessed 16 December 2019).
17. B. M. Lee et al. US Patent No. 5973139A (26 October 1999).
18. https://www.fujifilmusa.com/shared/bin/FAQs_DMP-2800_Series_Printer_DMC-11600+Series+Cartridge.pdf (accessed 16 December 2019).
19. Y. Sakai et al., *Sensor Actuat. B-Chem.* 35, 85-90 (1996).
20. S. A. Carvajal and C. A. Sánchez, *Int. J. Metrol. Qual. Eng.* 9, 9 (2018).
21. A. Oprea et al., *Sensor Actuat. B-Chem.* 132, 404-410 (2008).
22. A. V. Manishev et al., *P. IEEE* 92, 808-845 (2004).
23. *Gis Sol.* 2013. The state of the soils in France. A synthesis/Groupement d'intérêt scientifique sur les sols, France, (2014).
24. U. Altenberend et al., *Sens. Actuators B Chem.* 187, 280-287, (2013).
25. E. Zampetti et al., *Sens. Actuators B Chem.* 155, 768-774, (2011).
26. A. H. Bedane et al., *Adsorption* 20, 863 (2014).
27. V. Ducéré et al., *Sens. Actuators B Chem.* 106, 331-334, (2005).
28. R. Kohler et al., *Compos. Interface* 10, 255-276, (2003).
29. I. Bernacka-Wojcik et al., *Small* 15, 1902189, (2019).
30. X. Li et al., *Catena* 60, 227-237 (2005).
31. R. B. Thompson et al., *Soil Sci. Soc. Am. J.*, 71, 1647-1657 (2007).
32. A. M. A. Amer, *Wetting and Wettability (BoD – Books on Demand, 2015)*, p. 4.